

Measurements of the stagnation pressure in the center of a cavitating jet

A. J. Nobel · A. M. Talmon

Received: 12 April 2011/Revised: 16 October 2011/Accepted: 8 November 2011/Published online: 25 November 2011
© The Author(s) 2011. This article is published with open access at Springerlink.com

Abstract The stagnation pressure at a certain distance from the nozzle is important for the erosion/ cutting capacity of a submerged jet in dredging. The decay of the stagnation pressure with jet distance is well known in the case of non-cavitating jets. It is also known that cavitation causes the rate of decay to decrease. Under conditions of cavitation, a cone of bubbles forms around the jet, which decreases the momentum exchange between the jet and the ambient water and the associated entrainment. Despite the amount of research on cavitating jets, the literature does not provide a description for the entrainment in the case of a cavitating jet. Also, a useful description of the stagnation pressure decay of a cavitating jet is missing. To fill this lacuna, we carried out jet tests at various ambient pressures in both fresh and saline water. We present and analyse the results in this paper.

1 Introduction

In dredging-related projects, moving jets are widely used to excavate sediments from the seabed. In non-cohesive sediments (e.g. sands), grains are eroded from the bed by

the shear stresses exerted by jet flow: the higher the shear stresses, the higher the erosion velocity.

In cohesive sediments (e.g. clays), the shear stresses exerted by the jet are too small to erode these sediments. Cohesive sediments fail when the shear stresses in a slip-surface exceed the undrained shear strength (c_u) of these sediments. To erode/cut a cohesive sediment, the stagnation pressure exerted by a jet must be at least $6.4 c_u$ (Nobel et al. 2010).

Both the shear stresses and the stagnation pressure exerted by the jet are functions of the jet velocity. Thus, the velocity development with jet distance is of importance for the erosion capacity of a jet. The velocity development of a non-cavitating jet is well known, see e.g. (Rajaratnam 1976). Despite the amount of research on cavitating jets, the literature does not provide a description of the velocity and stagnation development of a cavitating jet. It is known that under conditions of cavitation, the decay of the stagnation pressure decreases with jet distance (Yahiro and Yoshida 1974; Soyama and Lichtarowicz 1996). There are only three datasets found of measurements on the stagnation pressure of cavitating jets.

Yahiro and Yoshida (1974) studied the influence of an air film around a submerged jet on the stagnation pressure decay. In the context of their study, they also conducted a lot of measurements on cavitating jets without an air film. The influence of cavitation on the stagnation pressure decay measured by Yahiro and Yoshida is much more significant than the influence reported in this paper. We have not found a convincing explanation for this difference. Other researchers on the influence of an air film around a jet also found a discrepancy between their datasets and that of Yahiro and Yoshida (Berg et al. 2006; Vinke 2009).

Shen and Sun (1988) studied the stagnation pressure decay of a submerged non-free jet. Although the jet

A. J. Nobel (✉) · A. M. Talmon
Department of Dredging Engineering,
Delft University of Technology, Delft, The Netherlands
e-mail: A.J.Nobel@tudelft.nl

A. J. Nobel
Royal Boskalis Westminster N.V., Papendrecht,
The Netherlands

A. M. Talmon
Deltares, Delft, The Netherlands
e-mail: A.M.Talmon@tudelft.nl

pressures were such that the jets should have been cavitating, the researchers do not mention the influence of cavitation. The trends they found are the same as those presented in this paper.

Soyama and Lichtarowicz (1996) investigated the structure of a cavitating jet, by measuring the stagnation pressure in the center and at different radial distances. Also, numerous high-speed recordings of the cavitating jets were taken. The main interest of this work was to correlate the stagnation pressure measurements with previously measurements on the maximum erosion rate of cavitating jets. Stagnation pressures are published at different jet distances and ambient pressures (0.16–0.4 MN/m²) for a cylindrical nozzle with a diameter of 2.5 mm and a jet pressure of 8 MN/m². They provide empirical equations for the length of the visible cavitation cone length, optimum stand off distance for erosion. The constants in the latter equations are not quantified.

Measurements on cavitating jets are usually restricted to their erosion rates and cutting capacities. For many materials, the cutting depths and/or productions are published as functions of various jet parameters. Usually, the erosion rate is based on free submerged cavitating jets impinging a surface perpendicular to the jet direction. In this case, the erosion rate is largely determined by the implusions of cavitation bubbles. The erosion rate is quite different from the erosion capacity of a moving jet penetrating cohesive soil.

In the case of a moving jet penetrating soil, the jet is partly enclosed by soil and only a small part at the front of the jet is used for cutting, see Fig. 1. It is assumed that the amount of cavitation bubbles at the interface is negligible, because the distance of the nozzle with respect to the undisturbed soil surface is relatively small. As a result, the direct contribution of bubble implusions on the erosion capacity is also assumed to be negligible.

In this case, cavitation increases the penetration depth of the jet. The cavitation bubbles at the back side of the jet decrease the entrainment, and as a result, the flow

velocities and stagnation pressures at the front side decay at a slower rate.

In order to determine a description for the entrainment of a cavitating jet, we carried out jet tests at various ambient fluid pressures in both fresh and saline water. We present and analyse the results in this paper.

1.1 Cavitation

The velocity difference between a jet and the ambient water creates a mixing layer in which the transfer of mass and momentum takes place. Ambient water is entrained in the jet, which decreases the static pressure around the jet. The higher the jet velocity, the more water entrained and the greater the pressure drop. Turbulent vortices locally further reduce the static pressure.

Vapor is formed inside the water when the static pressure drops below the vapor pressure (p_v). This can occur only at free surfaces. In natural water, free surfaces are normally present as micron-sized bubbles of contaminant gas called *nuclei*; these can be present in crevices within the solid boundary or within suspended particles or be freely suspended within the water. Typical nucleus radii are between 5 and 100 μm (Brennen 1995).

Because of the surface tension of the water (S), the exact critical ambient pressure ($p_{a,c}$) at which a micro-sized bubble is unstable, and will grow explosively, is often a little lower than the vapor pressure. For this study, the critical ambient pressure was assumed to be equal to the vapor pressure. Hence, the required pressure drop for cavitation (Δp_a) is about $p_{a0} - p_v$, where p_{a0} is the initial ambient fluid pressure.

In addition, the required pressure drop must persist for a period that is longer than the response time of the bubble, namely the time the bubble takes to grow to its critical diameter (Ooi 1985).

1.1.1 Incipient cavitation

Besides the research on the cutting capacity of a cavitating jet, research has also concentrated on incipient cavitation. Cavitation inception is defined as the moment that at least five bubbles expand and then implode (Ooi 1985). The conditions for cavitation inception are typically indicated by the cavitation inception index:

$$\sigma_i = \frac{p_{a0} - p_v}{1/2\rho u_0^2} \quad (1)$$

where ρ is the liquid density and u_0 the jet velocity at nozzle exit. The published cavitation inception numbers for submerged jets differ significantly. A collection of measured indices for untreated water shows values between 0.12 (Lienhard and Stephenson 1966) and 1.62 (Ran and

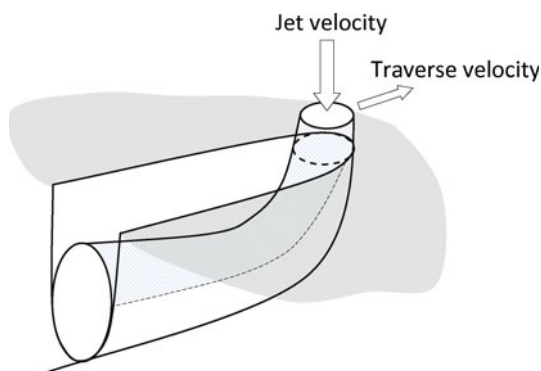


Fig. 1 Sketch of a moving jet penetrating cohesive soil

Katz 1994). This means that the static pressure fluctuations in the jet can reach a value of 1.62 times the dynamic head of the jet pressure at nozzle exit. Two trends are found: σ_i increases with nozzle diameter and with air content. Other trends are conflicting (Gopalan et al. 1999). An insufficient understanding of the underlying flow makes it difficult to interpret all differences.

It has been determined that the first cavitation bubbles do not influence the jet flow and the jet cutting production. Hence, the exact value of σ_i is of little relevance to the cutting of cohesive sediments. What is more relevant is the condition: cavitation influences the maximum stagnation pressure firstly, which is expressed in the cavitation number of cone development:

$$\sigma_d = \frac{p_{a0} - p_v}{p_{cav}} \approx \frac{p_{a0}}{p_{cav}} \quad (2)$$

where p_{cav} is the *jet pressure for cavitation cone development*, defined as the lowest jet pressure (pressure difference) at which the influence of cavitation on the stagnation pressure is measurable. The value of σ_d is necessarily smaller than σ_i . However, no σ_d values are given in the literature. This paper presents such values for various nozzle diameters and ambient pressures.

1.1.2 Developed cavitation

When the pressure drop required for cavitation is about constant and extends over a long distance, a cone of cavitation bubbles forms around the jet. The jet core remains free of cavities (Ran and Katz 1994). This cone reduces the exchange of momentum between the jet and the ambient water. As a result, less ambient water is entrained and the decrease in jet velocity and stagnation pressure with distance is reduced.

With an increase in jet pressure, the pressure drop required for cavitation extends over a longer distance. Hence, the length of the cone increases with jet pressure.

The structure of a cavitating jet and the behavior of unsteady cavitation bubbles are still unclear. In addition, modeling numerically a cavitating jet is very challenging. In the cavitation region, the flow is compressible, while in the non-cavitating regions, the flow is incompressible. Although a number of attempts have been made to model a cavitating jet, see e.g. Xing and Frankel (2002), Peng and Fujikawa (2006) and Alehossein and Qin (2007), an integral model is not yet available.

2 Experimental setup

Cavitating jet tests were carried out in a 1.6-m-long, 1.2 m diameter cylindrical pressure vessel (see Figs. 2 and 3). A

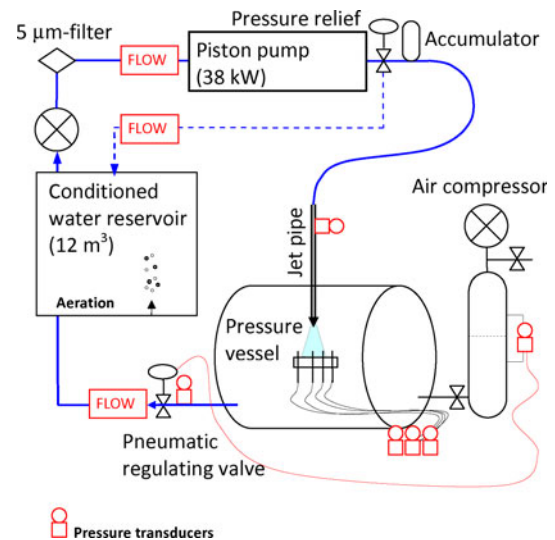


Fig. 2 Experimental set-up



Fig. 3 Overview of experimental set-up (Deltares Delft)

height-adjustable vertical jet pipe was installed on the top of this vessel. The vertical and horizontal position of the jet could be adjusted above the measuring panel within a tenth of a millimeter.

The jet flow was provided by an electrically operated, frequency-regulated piston pump (38 kW). The maximum jet flow was 235 l/min. The flow could be reduced by means of a pressure relief valve in the bypass at the discharge side of the pump. The pressure peaks of the three pistons were damped by an accumulator.

The ambient pressure in the vessel was adjusted with a regulating valve in the drain. The pressure fluctuations in the vessel were damped by a large accumulator (50 l) behind the vessel.

2.1 Measuring panel

The measuring panel, which was located in the middle of the vessel, was designed such that it disturbed the jet only minimally. This panel consisted of a structure in which eight very thin (OD 1.58 mm) hollow tubes were clamped vertically along the two axes (see Fig. 4). These tubes were the measuring points for the stagnation pressure and were connected to separate (calibrated) pressure transducers. The range of the used pressure transducers was matched to the expected stagnation pressures.

2.2 Nozzles

Most tests were carried out with short nozzles of the brand Woma. Three nozzle diameters (D_n) were tested: 3, 5 and 7 mm (see Fig. 5).

These nozzles were relatively short, which results in low discharge coefficients, defined as the jet flow divided by the nozzle surface multiplied by the jet velocity; $\mu_n = Q_0 / (A_n u_0)$. The calculated discharge coefficients of these nozzles were 0.89, 0.88 and 0.89, respectively. To investigate the influence of nozzle design on the cavitation behavior, also, a long conical nozzle was tested. The calculated discharge coefficient of this nozzle was significantly higher 0.99.

In almost the same experimental setup, the influence of an air film around a jet was investigated (Berg et al. 2006)¹. The results of reference tests with this nozzle, without air, are included in the analysis. The nozzle was designed according to Yahiro and Yoshida (1974) and is therefore called the *Yahiro-nozzle*. Its nozzle diameter was 3 mm, and it had a discharge coefficient of 0.82.

2.3 Test settings

Table 1 presents the test settings. Where the jet pressure (p_{jet}) is defined as the pressure difference between the absolute upstream pressure (p_{up}) and the initial ambient fluid (downstream) pressure (p_{a0}).

To ensure that the water properties were constant, continually aerated and filtered (5 μm) tap water was used. Some tests were carried out with saline water. A solution of NaCl was added to tap water to produce saline water. The measured salinity was about 42‰ (which is a little higher than that of normal seawater, i.e. 35‰) (Table 2).

3 Repeatability and accuracy measurements

To verify the repeatability of the measurements, some test settings were repeated at the end of many test series. There

¹ This air was externally supplied by a compressor.

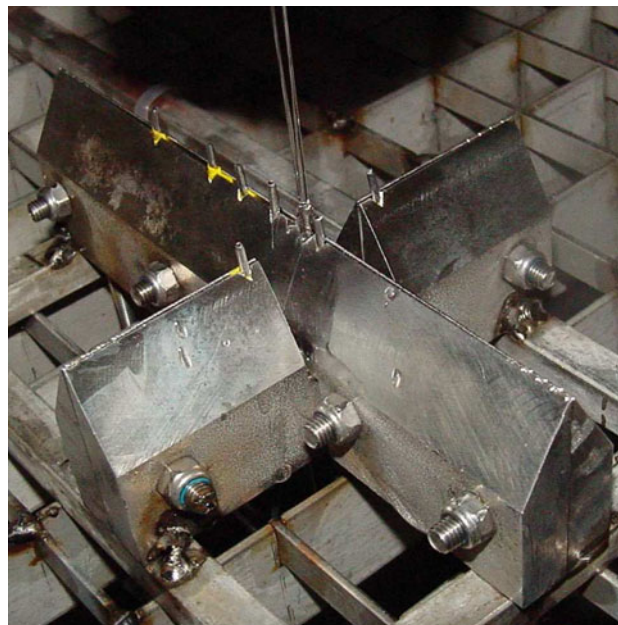


Fig. 4 Measuring panel for the stagnation pressure

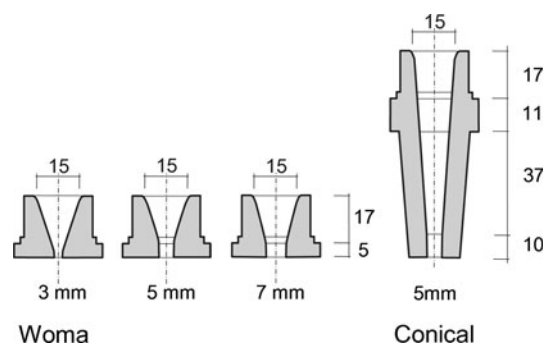


Fig. 5 Dimensions used nozzles

Table 1 Test settings

Jet pressure	1.5–20 (MN/m ²)
Nozzle diameter	3, 5 and 7 (mm)
Standoff distance	6–72 D_n (mm)
Ambient pressure	0.10–0.57 (MN/m ²)

Table 2 Water properties

Air content	10–12 (ppm)
Water temperature	12–15 (°C)
Nuclei diameter	<5 (μm)
Salinity	0 & 42 (‰)

was also some overlap in test settings in different test series. The maximum difference in measured stagnation pressures is of the order of 10%, as can be noticed in some of the figures.

It was found that at high jet pressures ($>15 \text{ MN/m}^2$) the jet pipe shifted minutely. In these cases, the center line stagnation pressure was obtained, in back-analysis, by shifting the nozzle position fictitious such that all eight measured stagnation pressures lay on a symmetric profile (close to Gaussian).

The tests into the influence of an air film around the jet were carried out some months later in the same pressure vessel (Berg et al. 2006). All sensors were re-connected, the measuring panel was adapted, an air-inlet was provided and the Yahiro-nozzle was mounted. The jetpipe was fixated better than during previously test series. Also the alignment of the nozzle was checked regularly by shifting the nozzle a little in the horizontal plane to find the highest stagnation pressure.

The results of reference tests without air film showed the same trends. Because of a different nozzle design, the absolute values of the measured stagnation pressures were slightly different, see ‘‘Sect. 4.3’’, Fig. 9.

The measured stagnation pressures of present study globally correspond with the data of Shen and Sun (1988) (see Fig. 7) and Soyama and Lichtarowicz (1996) (see Figs. 12, 18).

4 Results

The presented stagnation pressures (p_{stag}) and jet pressures (p_{jet}) are defined with respect to the initially ambient fluid pressure:

$$p_{\text{stag}} = p_m - p_{a0} \tag{3}$$

$$p_{\text{jet}} = p_{\text{up}} - p_{a0} \tag{4}$$

where p_m is the measured absolute stagnation pressure in the center of the jet and p_{up} the measured absolute (upstream) pressure in the jetpipe.

4.1 Jet pressure

The stagnation pressures normalized with jet pressure for the three nozzle diameters are plotted in Fig. 6 as function of the jet pressure. These pressures were measured at a jet distance of $12D_n$ and an initially ambient fluid pressure (p_{a0}) of 0.13 MN/m^2 .

For a non-cavitating jet, the normalized stagnation pressure in the center of the jet can be calculated with the following equation:

$$\frac{p_{\text{stag,NC}}}{p_{\text{jet}}} = \frac{k}{2} \left(\frac{D_n}{s} \right)^2 \tag{5}$$

where s is the jet distance and k is an experimental constant. Fischer et al. (1979) found, based on 13 experimental

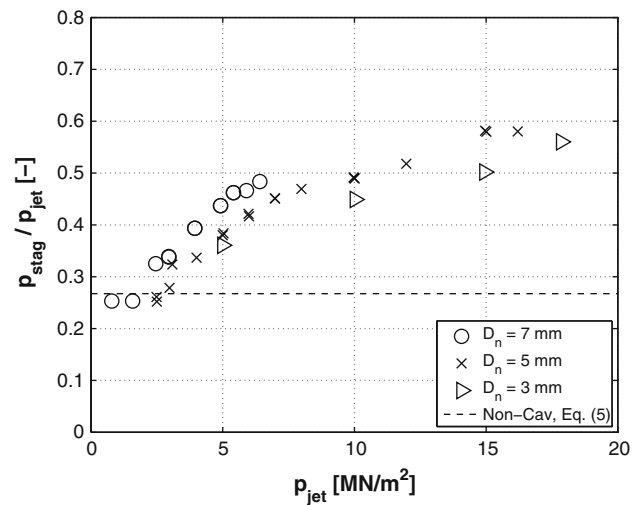


Fig. 6 Influence of nozzle diameter and jet pressure on the normalized stagnation pressure at an initial ambient fluid pressure of 0.13 MN/m^2 and a jet distance of $12D_n$

investigations, a value of 77 for k^2 . It follows that at a certain jet distance, the normalized stagnation pressure for a non-cavitating jet is independent of the nozzle diameter and jet pressure. At a jet distance of $12D_n$, the calculated normalized stagnation pressure is about 0.27 (striped line in Fig. 6).

At a jet pressure of about 2.5 MN/m^2 , the normalized stagnation pressures start to increase. At this pressure, the cone of bubbles reduces the entrainment. This is an important pressure and is defined as the *jet pressure for cavitation cone development* (p_{cav}). The corresponding cavitation number for cone development (σ_a) is 0.052.

At higher jet pressures, more and more cavitation bubbles are formed. As a result, the effectiveness of the cone of bubbles increases and the direct interaction surface between the jet and ambient fluid shrinks. This interaction area is responsible for the exchange of momentum between the jet and the ambient water, and thus for cavitation. A reduction in this area results in a decrease in the momentum exchange and in the static pressure drop.

At a certain jet pressure, the effectiveness of the cavitation cone, expressed in the normalized stagnation pressure, reaches a maximum value. A further increase in jet pressure results only in a negligible increase in the normalized stagnation pressure. The number of newly formed bubbles per interaction area is optimized/maximized.

Shen and Sun (1988) measured the stagnation pressure with a pitot tube in a jet with a nozzle diameter of 2.85 mm. They found the same trend, see Fig. 7. The increase in the normalized stagnation pressure for the 2.85-mm nozzle is stronger than for the 3-mm nozzle we used.

² The published values of constant k range from 72 to 115, see also (Fondse et al. 1983).

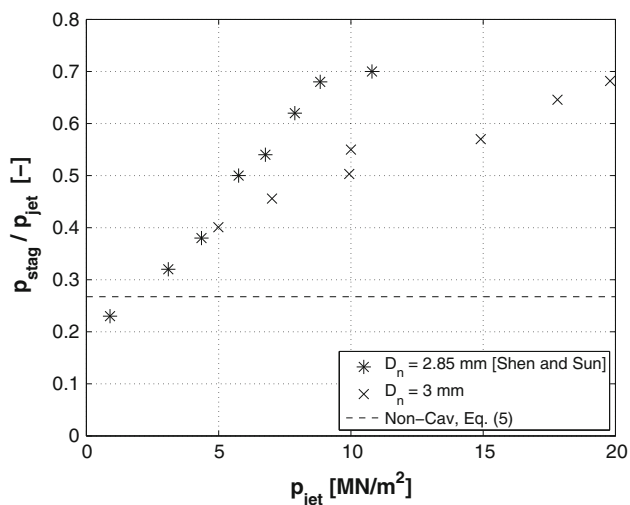


Fig. 7 Comparing the normalized stagnation pressures measured by Shen and Sun (1988) and present results for the 3-mm nozzle at an initial ambient fluid pressure of 0.1 MN/m² and a jet distance of 36 mm

The exact explanation for this difference cannot be given. Probably the difference can be partly explained by the difference in nozzle design, see Sect. 4.3.

4.2 Nozzle diameter

As shown in Fig. 6, the differences between the three nozzle diameters are limited. Table 3 presents p_{cav} and corresponding σ_d for the nozzles. The jet pressures for cavitation cone development increase with nozzle diameter. The same trend was found for the cavitation inception number. Cavitation inception numbers for similar nozzle diameters measured by Ooi (1985) are listed in Table 4. Necessarily, the value of $\sigma_d < \sigma_i$. Also, the calculated critical jet pressures for cavitation inception ($p_{cav,i}$) at an ambient pressure of 0.13 MN/m² are listed. These pressures are significantly lower than the pressures for cavitation cone development.

4.3 Nozzle design

The Figs. 8 and 9 show the influence of nozzle design on the normalized stagnation pressure. The normalized

Table 3 Jet pressures for cavitation cone development and the corresponding cavitation numbers for the three nozzle diameters ($p_{a0} = 0.13 \text{ MN/m}^2$)

D_n (mm)	p_{cav} (MN/m ²)	σ_d (-)
7	2	0.065
5	2.4	0.055
3	2.6	0.050

Table 4 Cavitation inception numbers measured by Ooi (1985) and calculated critical jet pressures for cavitation inception at an ambient pressure of 0.13 MN/m² (air content 10.5 ppm)

D_n (mm)	σ_i (-)	$p_{cav,i}$ (MN/m ²)
6.35	0.24	0.54
4.76	0.11	1.2
3.17	0.08	1.6

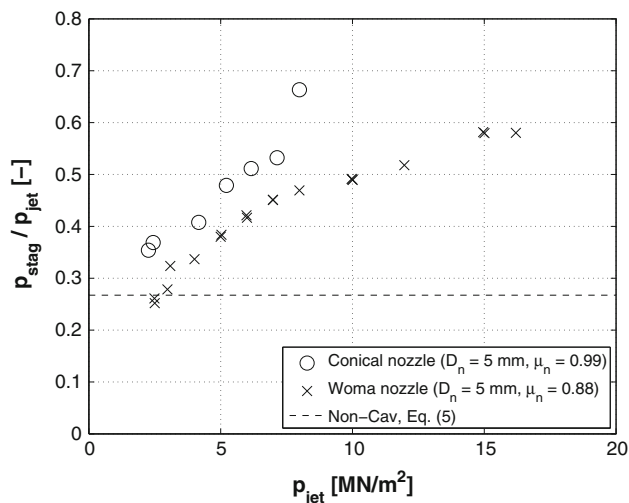


Fig. 8 Influence of nozzle design on the normalized stagnation pressure at an initial ambient fluid pressure of 0.13 MN/m² and a jet distance of $12D_n$

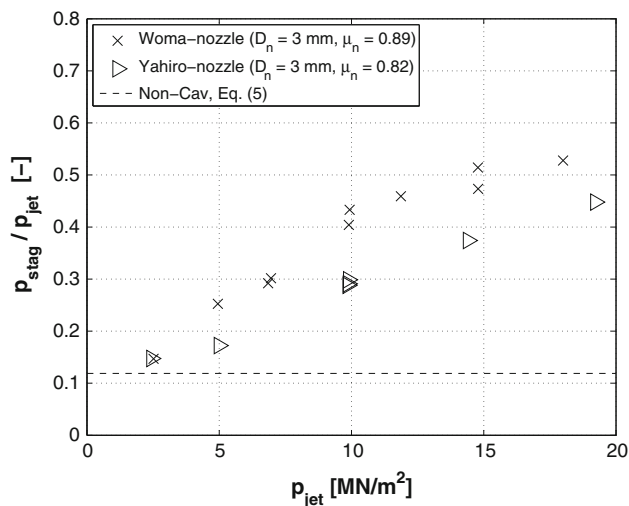


Fig. 9 Influence of nozzle design on the normalized stagnation pressure at an initial ambient fluid pressure of 0.13 MN/m² and a jet distance of $18D_n$

stagnation pressures of the conical nozzle are structurally higher. The comparison between the Woma-nozzle with the Yahiro-nozzle show a similar difference.

These differences can partly be explained by the differences in discharge coefficients; the higher the discharged coefficient the higher the normalized stagnation pressures. To discount the effect of nozzle design, it is better to normalize the jet distance with the initial jet diameter ($D_0 = \sqrt{\mu_n} D_n$) instead of the nozzle diameter. This was already suggested by Soyama and Lichtarowicz (1996).

4.4 Ambient pressure

The pressure drop required for cavitation (Δp_a) increases linearly with the ambient pressure. Thus, the jet pressures for cavitation cone development also increase with ambient pressure. Figure 10 shows the measured stagnation pressures normalized with jet pressure for the 5-mm nozzle at various ambient pressures as function of the jet pressure. These pressures were measured at a normalized jet distance of $12D_n$.

At all jet pressures, the normalized stagnation pressure decreases with ambient pressure. It is remarkable that the normalized stagnation pressures at certain conditions are lower than can be expected for a non-cavitating jet. This decrease is probably a result of imploding bubbles. Increasing the ambient pressure increases the impact of the implusions. The distortionary impact of these implusions on jet flow is apparently greater than the positive effect of the presence of bubbles.

The jet pressures of cavitation cone development (p_{cav}) and the corresponding σ_d at different ambient pressures are listed in Table 5. The differences between the cavitation numbers are limited. This means that the pressure for cone development increases approximately linearly with

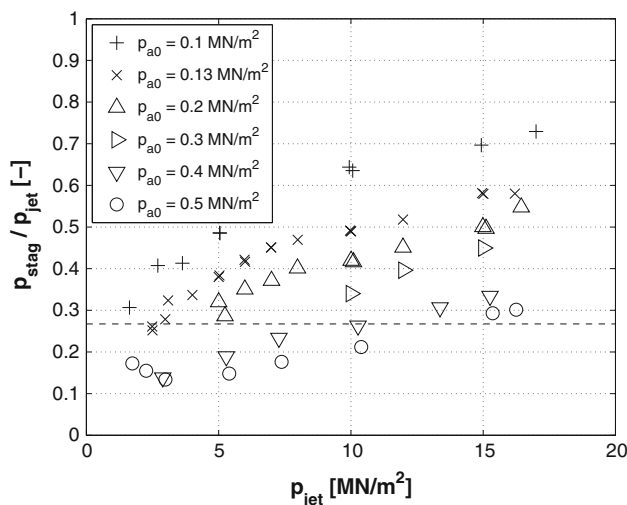


Fig. 10 Influence of ambient fluid pressure on the normalized stagnation pressure for the 5-mm nozzle at a jet distance of $12D_n$

Table 5 Jet pressures for cavitation cone development and the corresponding cavitation numbers for the 5-mm nozzle at different ambient pressures

p_{a0} (MN/m ²)	p_{cav} (MN/m ²)	σ_d (-)
0.1	1.5	0.067
0.13	2.4	0.055
0.2	3.5	0.057
0.3	6	0.05
0.4	9	0.044
0.5	11.5	0.043

ambient fluid pressure, see Fig. 11. The average value of σ_d is about 0.045.

4.5 Jet distance

Figure 12 shows the measured stagnation pressures normalized with jet pressure as function of jet distance for the 3-mm nozzle. These pressures are measured at an ambient pressure of 0.13 MN/m^2 . As a reference, the normalized jet pressures for a non-cavitating jet are also plotted (striped line).

The stagnation pressures published by Soyama and Lichtarowicz (1996) are also plotted in Fig. 12.³

The data show the same trend. The ambient fluid pressure was however a little higher (0.16 MN/m^2); therefore, the data are not fully comparable. The normalized stagnation pressures lie a little higher than one would expect on basis of present data.

To investigate the effectiveness of the cavitation cone, the measured stagnation pressures given in Fig. 13 are normalized with the calculated stagnation pressures for a non-cavitating jet ($p_{stag,NC}$, see Eq. 5). For a non-cavitating jet, the stagnation pressure in the center equals the jet pressure up to a jet distance of $\sqrt{k/2} D_n \approx 6.2D_n$. Thus, up to a jet distance of $6.2D_n$ no effect of cavitation can be measured ($p_{stag}/p_{stag,NC} = 1$). For all jet pressures, the effectiveness of the cavitation cone is maximal at a jet distance of about $18D_n$. For a jet pressure of 19.5 MN/m^2 , the measured stagnation pressure is almost 4 times higher than that calculated for a non-cavitating jet. At a jet distance of $18D_n$ and further, the effectiveness of the

³ Because the stagnation pressures are read from a figure the accuracy is not high. Soyama and Lichtarowicz (1996) measured the stagnation pressure on a plate orientated perpendicular to the main flow direction. In such a flow, the jet is disturbed downstream from about 0.86 times the standoff distance (Rajaratnam 1976). This means that the real stagnation point lie about 0.14 times the standoff distance before the plate. In the present study, the jet flow was disturbed minimally at the measuring points. To compensate for this, the jet distance (s) given by Soyama and Lichtarowicz (1996) was corrected with a factor 0.86.

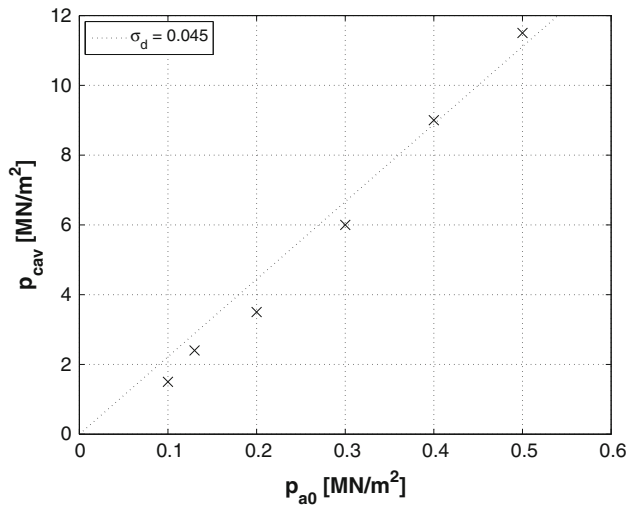


Fig. 11 Jet pressures for cavitation cone development as function of the ambient fluid pressure for the 5-mm nozzle at a jet distance of $12D_n$

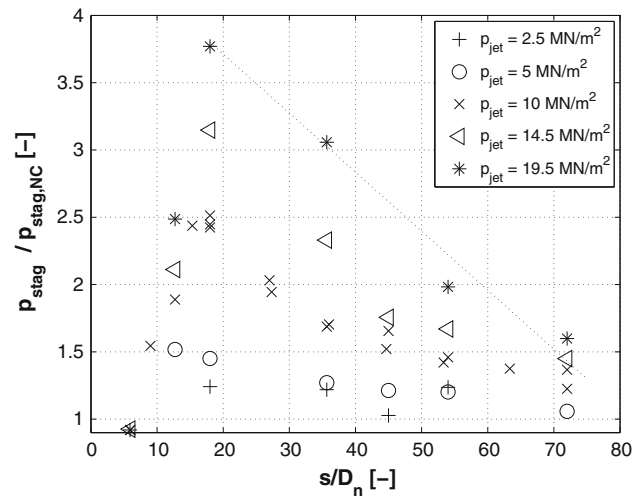


Fig. 13 Effectiveness of cavitation cone ($D_n = 3$ mm, $p_{a0} = 0.13$ MN/m²)

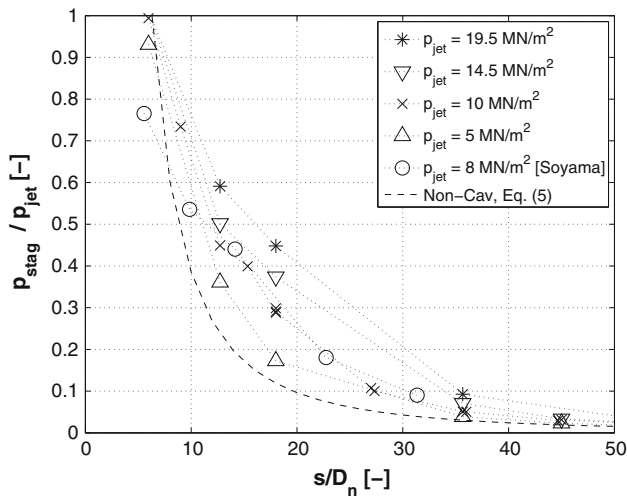


Fig. 12 Influence of jet distance on the normalized stagnation pressure for the 3-mm nozzle at a ambient fluid pressure of 0.13 MN/m²

cavitation cone decreases almost linearly with jet distance (see dotted line). This decrease is also due to the limited length of the cone. At a certain jet distance, the jet velocity has decreased such that no new bubbles are formed.

4.6 Salinity

In dredging practice, jetting mostly takes place in seawater that has a salinity (c_s) of about 35‰. Cavitation-determining parameters namely vapor pressure (p_v) and surface tension (S) differ a little with salinity (see Table 6). The nuclei distribution is also different. A typical nuclei distribution measured in the Pacific Ocean shows that the

Table 6 Vapor pressure and surface tension of fresh water ($c_s = 0‰$) and saline water ($c_s = 35‰$)

T (°C)	p_v (kN/m ²)		$S \cdot 10^{-2}$ (N/m)	
	$c_s = 0‰$	$c_s = 42‰$	$c_s = 0‰$	$c_s = 35‰$
10	1.23	1.21	7.42	7.49
20	2.34	2.30	7.28	7.35

number of nuclei with radii <20 μm is much higher than the number for fresh water (O’Hern et al. 1988).

To investigate the influence of salinity on cavitation, we carried out some jet tests in water with a 42‰ salinity. Figure 14 shows the measured stagnation pressures normalized with jet pressure for fresh and saline water. The nozzle diameter was 5 mm, the jet distance $12D_n$ and the ambient pressure 0.13 MN/m². The differences between the pressures in fresh and saline water are negligible. For more developed cavitation, the influences of the differences in p_v and S for fresh and saline water are apparently negligible.

Another difference between fresh and saline water is the susceptibility of the bubbles to coalesce. In fresh water, bubbles tend to coalesce and form large bubbles. In saline water, free surfaces are slightly negatively charged. The resulting electrical repulsive forces prevent bubbles for coalescing (Weissenborn and Pugh 1995). Hence, in saline water, the cavitation bubbles remain relatively small.

Due to their buoyancy, the bubbles will rise and escape the cone of cavitation bubbles. Because the buoyancy of the bubbles increases with volume, they rise and escape the cone earlier in fresh water than in saline water. Hence, the effective length of the cavitation cone in saline water is possibly greater than in fresh water. This is confirmed by jet tests executed by Summers and Sebastian (1980).

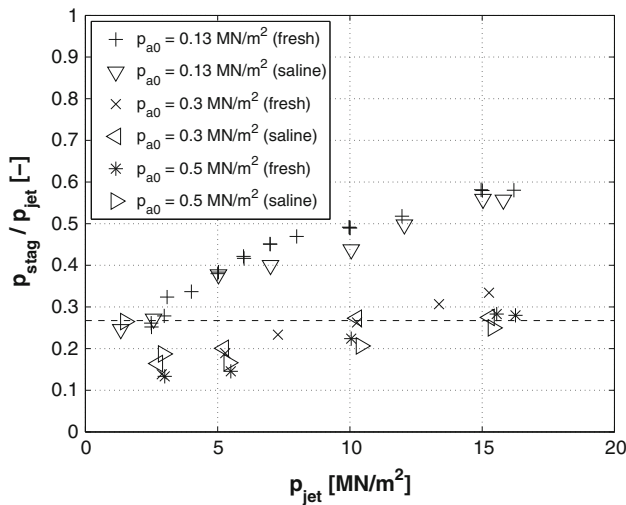


Fig. 14 Results for fresh water ($c_s = 0\%$) and saline water ($c_s = 42\%$) ($D_n = 5$ mm, $s/D_n = 12$)

During some tests, the cavitation cone was captured with a high-resolution video camera. These images allowed the length of the cavitation cone to be measured. Table 7 presents the measured lengths of the cavitation cone under similar test conditions in fresh and saline water. The differences are negligible.

5 Analyses

5.1 Development of stagnation pressure

Under conditions of cavitation, a cone of bubbles forms around the jet, which decreases the momentum exchange between the jet and the ambient fluid. The effectiveness of the cavitation cone depends on the quantity and radii of the cavitation bubbles. The thickness of the cavitation cone layer is not constant over the full length of the cone (see Fig. 15). Soyama and Lichtarowicz (1996) provided a comparable sketch describing the shift of the contour of a cavitating jet in comparison with a non-cavitating jet.

The cone needs to develop over some length; this is called the cone development region. Both the number of

Table 7 Measured length of the cavitation cone (L_{cone}) in fresh and saline water ($D_n = 5$ mm)

p_{jet} (MN/m ²)	p_{a0} (MN/m ²)	L_{cone} (mm)	
		$c_s = 0\%$	$c_s = 42\%$
2.5	0.13	98	110
2.5	0.5	38	32
5	0.5	62	60

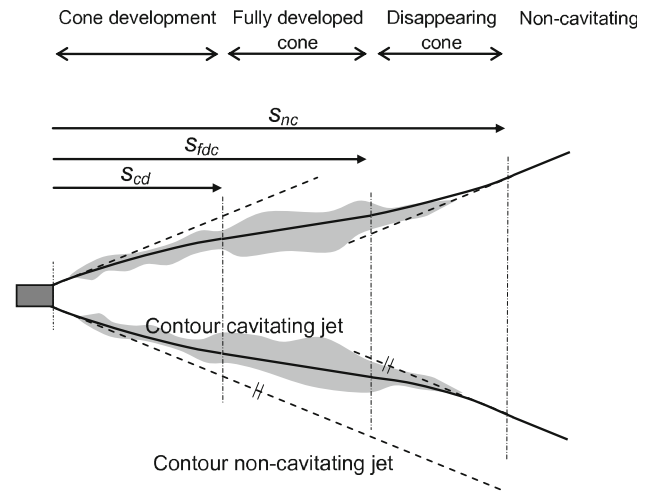


Fig. 15 Definition sketch of the various developing regions of the cavitation cone

bubbles per unit length and their radii increase in this region. After this region is a second region, in which the cone is fully developed and the effectiveness is roughly constant. The length of this region depends on the jet pressure, ambient pressure and nozzle diameter. At a certain distance, the jet velocity decreases such that the conditions for cavitation are no longer satisfied and no new bubbles are formed. The cavitation cone loses its effectiveness and disappears, after which the entrainment per unit length equals the entrainment of the non-cavitating jet.

When the cavitation cone is fully developed, the entrainment per unit length is roughly constant and can be expressed by the following equation (similar with a non-cavitating jet):

$$\frac{dQ}{ds} = \frac{1}{\sqrt{2k_{cav}}} \pi D_n u_0 = \alpha_{mom,cav} \pi D_n u_0 \tag{6}$$

where k_{cav} is an empirical constant and $\alpha_{mom,cav}$ is the entrainment coefficient. The larger k_{cav} , the more the entrainment is reduced. For a non-cavitating jet, $k \approx 77$ (Fischer et al. 1979). It is assumed that for jet pressures below the pressure for cavitation cone development (p_{cav}), the influence of cavitation is negligible ($k_{cav} = k$), and that for jet pressures above p_{cav} , the value of k_{cav} increases with $\sqrt{p_{jet}/p_{cav}}$. With $p_{cav} = 1/\sigma_d \cdot p_{a0}$ (see Sect. 4), the empirical constant for a developed cavitation cone k_{cav} can be written as:

$$k_{cav} = k \sqrt{\sigma_d} \sqrt{\frac{p_{jet}}{p_{a0}}} \tag{7}$$

This results in the following relation for the entrainment coefficient:

$$\alpha_{\text{mom,cav}} = \sqrt{\frac{1}{2k}} \sqrt[4]{\frac{p_{a0}}{\sigma_d p_{\text{jet}}}} \quad (8)$$

Substituting $k = k_{\text{cav}}$ into Eq. 5 results in the following relation for the normalized stagnation pressure ($p_{\text{jet}} > p_{\text{cav}}$):

$$\frac{p_{\text{stag}}}{p_{\text{jet}}} = \frac{k}{2} \sqrt{\sigma_d} \sqrt{\frac{p_{\text{jet}}}{p_{a0}}} \left(\frac{D_n}{s}\right)^2 \quad (9)$$

5.2 Measured versus calculated stagnation pressures

The measured and the calculated normalized stagnation pressures (Eq. 9) are plotted in Fig. 16 as function of the jet pressure. The jet distance is $12D_n$ and the nozzle diameter is 5 mm. The values for k and σ_d are 77 and 0.045, respectively. The measured and the calculated normalized stagnation pressures are in good agreement with each other.

Figure 17 shows all measured stagnation pressures for the 5-mm nozzle at a distance of $12D_n$ according to Eq. 9. The correlation is quite good.

The measured stagnation pressures for the Yahiro-nozzle and the obtained stagnation pressures from Soyama and Lichtarowicz (1996) are plotted in Fig. 18 in the same way as in Fig. 17. As a reference, the estimated values (according to Eq. 9) are also plotted (striped line). Again the value of σ_d is 0.045, but for k , a value of 95 is used. This value results in a better correlation than the previously used value of 77. A value of 95 is not unrealistic. Depending on the outlet conditions of the jet, values up to 115 are mentioned, see Fondse et al. (1983).

All data points obtained by Soyama and Lichtarowicz (1996) lie a little above the reference line. Probably this is

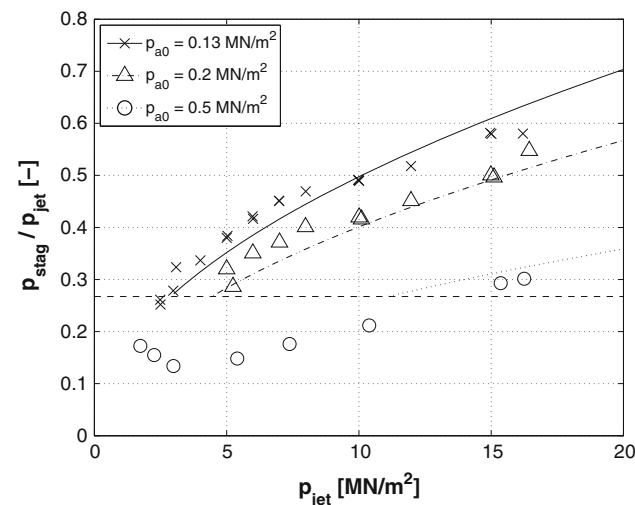


Fig. 16 Measured (Eq. 9; $\sigma_d = 0.045$, $k = 77$) and calculated normalized stagnation pressures as function of the jet pressure for different ambient pressures ($D_n = 5$ mm, $s/D_n = 12$)

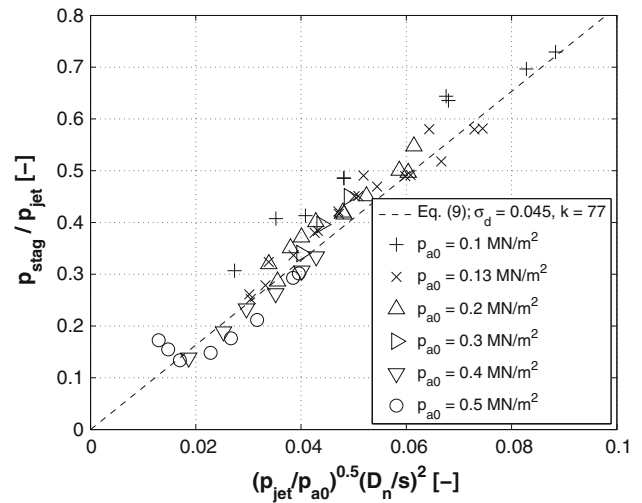


Fig. 17 Correlation according to Eq. 9 ($D_n = 5$ mm, $s/D_n = 12$)

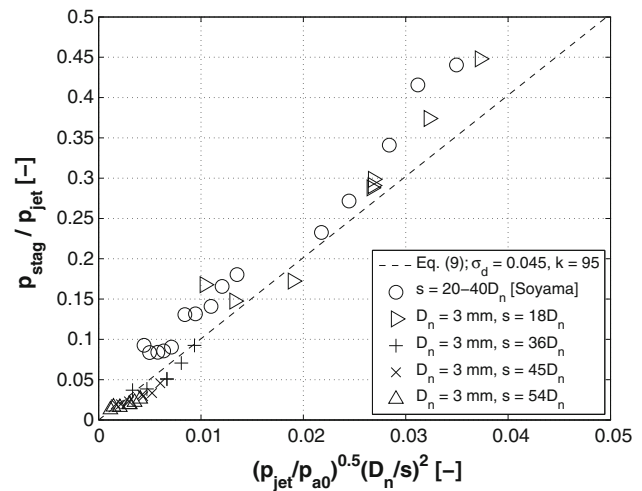


Fig. 18 Correlation according to Eq. 9 for the Yahiro-nozzle ($D_n = 3$ mm, $p_{a0} = 0.13$ MN/m²) and the data obtained from Soyama and Lichtarowicz (1996) ($D_n = 2.5$ mm, $p_{a0} = 0.16$ – 0.4 MN/m²)

due to the differences in nozzle geometry. By increasing the value of k a little, a better correlation will be found.

The values of the Yahiro-nozzle measured at long jet distances are beneath the reference line (data points located near the origin), which means that the stagnation pressures calculated by equation Eq. 9 are slightly overestimated. This can be explained by a decrease in the effectiveness of the cavitation cone at long distances. Equation 9 assumes a constant effectiveness over the whole jet distance.

5.3 Effective length cavitation cone

Equation 9 is valid only in the fully developed cone region. This region starts at a jet distance where $p_{\text{stag}}(s_{cd})$ equals p_{jet} :

$$\frac{s_{cd}}{D_n} = \sqrt{\frac{k}{2}} \sqrt{\frac{\sigma_d p_{jet}}{p_{a0}}} = \frac{1}{2\alpha_{mom,cav}} \tag{10}$$

In the cone development region, the stagnation pressure in the center of the jet equals the jet pressure ($s < s_{cd}$: $p_{stag} = p_{jet}$).

It is difficult to estimate the length of the fully developed cone region. The jet conditions for which no new bubbles are formed are unknown. It was initially assumed that the jet pressure for cavitation cone development (p_{cav}) is also the minimum pressure required for the formation of new bubbles. In this case, the fully developed cone region ends when the maximum stagnation is decreased to the value of p_{cav} . The jet distance that satisfies this condition can be calculated with Eq. 9. It follows that:

$$\frac{s_{fdc}}{D_n} = \sqrt{\frac{k}{2}} \sigma_d^{1.5} \left(\frac{p_{jet}}{p_{a0}}\right)^{1.5} \approx C_{fdc} \sigma^{-0.75} \tag{11}$$

where C_{fdc} is an empirical constant, depending on the nozzle geometry. For the used nozzle, the value of C_{fdc} range from about 0.6 to 0.67.

Assuming that the influence of the cone on the momentum exchange in the disappearing cone region is negligible, Eq. 9 is valid from s_{cd} to s_{fdc} . For jet distances $> s_{fdc}$, the value of the entrainment coefficient is the same as for a non-cavitating jet. At these distances, the influence of cavitation can be taken into account by introducing a fictitious displacement (Δs) in Eq. 5 (see Fig. 19):

$$s > s_{fdc}$$

$$p_{stag} = \frac{k}{2} p_{jet} \left(\frac{D_n}{s - \Delta s}\right)^2 \tag{12}$$

$$\Delta s = \sqrt{\frac{k}{2}} \sigma_d \frac{p_{jet}}{p_{a0}} \left(\sqrt{\frac{\sigma_d p_{jet}}{p_{a0}}} - 1\right) D_n$$

The calculated normalized stagnation pressures, according to the above theory, for the Yahiro-nozzle are plotted in Figs. 20 and 21 as function of the normalized jet distances. As a reference, the measured values are also

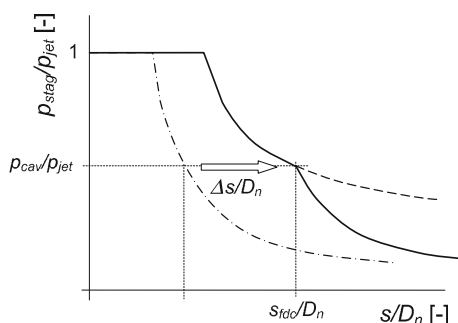


Fig. 19 Definition sketch of the shift in jet distance in the equation for the stagnation pressure of a non-cavitating jet to discount for the influence of cavitation

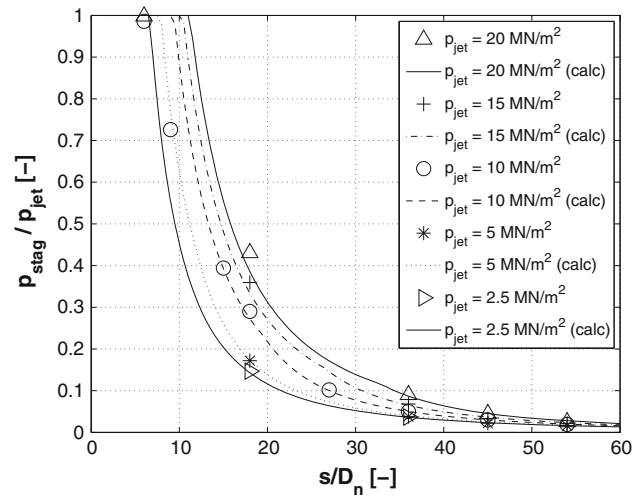


Fig. 20 Measured and calculated normalized stagnation pressures for the Yahiro-nozzle at an ambient pressure of 0.13 MN/m² ($D_n = 3$ mm, $k = 95$, $\sigma_d = 0.045$)

plotted. To fit the data also into the non-cavitating regime ($p_{jet} = 2.5$ MN/m²), a k -value of 95 is used (see the section above). All measured values (except that at a normalized jet distance of 9) are in good agreement with the calculated ones.

For a jet pressure of 20 MN/m², the fully developed cone region ends at a normalized jet distance of 33. Beyond the end of the fully developed cone region, the entrainment per unit length increases to the value of a non-cavitating jet, resulting in a stronger decrease in stagnation pressure with jet distance (see Fig. 21).

5.4 Visible length cavitation cone

In Table 8, some observations of the visible cone length (s_{nc}) are compared with the calculated distance of the end of the fully developed cone region (s_{fdc} , for definitions see Fig. 15). It appears that s_{fdc} is significantly shorter than s_{nc} . The visible cone is apparently not effective over the full length. This is consistent with the observation that even before any influence of cavitation on the stagnation pressure is measured ($p_{jet} < p_{cav} = 2.4$ MN/m²), already a cone is clearly visible.

It is found that the visible cone length corresponds with the condition $p_{stag} = 0.15 p_{cav}$, see Fig. 22:

$$\frac{s_{nc}}{D_n} = \sqrt{\frac{1}{0.15} \frac{k}{2}} \sigma_d^{1.5} \left(\frac{p_{jet}}{p_{a0}}\right)^{1.5} \approx C_{nc} \sigma^{-0.75} \tag{13}$$

where C_{nc} is an empirical constant. For the used nozzle, the value of C_{nc} range from about 1.57 to 1.74.

Soyama and Lichtarowicz (1996) found an identical type of relation for the visible cone length:

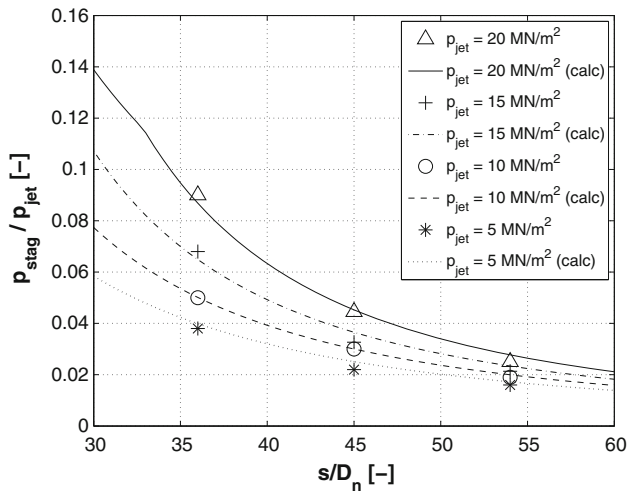


Fig. 21 Measured and calculated normalized stagnation pressures for the Yahiro-nozzle (close-up of Fig. 20)

Table 8 Comparison between the observed cavitation cone length (s_{nc}) and the calculated end of the fully developed cone region (s_{fdc}) for the 5-mm nozzle at an ambient fluid pressure of 0.13 MN/m^2

p_{jet} (MN/m^2)	s_{fdc} (mm)	s_{nc} (mm)
0.95	0	32
2.6	33	98
5.0	54	133
7.0	70	155

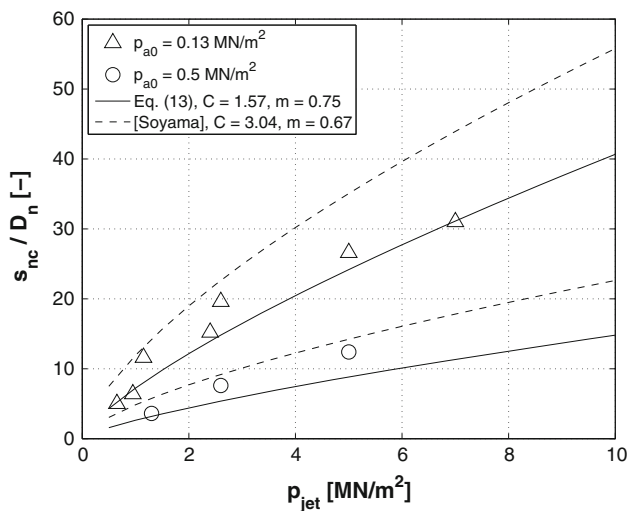


Fig. 22 Measured and calculated normalized visible cone length for the 5-mm nozzle at an ambient fluid pressure of 0.13 and 0.5 MN/m^2

$$\frac{s_{nc}}{D_n} = C_{nc} \sigma^{-m} \tag{14}$$

Table 9 shows the values found by Soyama and Lichtarowicz (1996) for the empirical constants C_{nc} and m , depending on the nozzle geometry. These values

Table 9 Empirical constants C_{nc} and m found by Soyama & Lichtarowicz (1996)

Type	C_{nc} (-)	m (-)
Cylindrical	1.73	0.83
Conical	3.04	0.67

produce a similar result as the values found in the present study, see also Fig. 22.

6 Conclusions

1. A non-cavitating jet is self-similar: the normalized stagnation pressure (p_{stag}/p_{jet}) is only a function of coordinates made dimensionless with the nozzle diameter. The stagnation pressure is independent of ambient pressure. For a cavitating jet, p_{stag}/p_{jet} decreases with ambient pressure.
2. The salinity of jet water and ambient water has a negligible influence on the behavior of a cavitating jet.
3. The increase in the stagnation pressure by cavitation is due to the development of a cone of cavitation bubbles around the jet, which decreases the momentum exchange and thus the entrainment of ambient water. An empirical formula for the entrainment coefficient, in the cavitation zone of a cavitating jet, is derived and verified with measurements.
4. After a certain jet distance, the cone of cavitation bubbles disappears and the entrainment coefficient decreases to the value of a non-cavitating jet. At these distances, the influence of cavitation can be taken into account by adding a fictitious displacement (Δs) in the standard equation for a non-cavitating jet. Based on measured stagnation pressures, an equation for Δs is derived.
5. The length of visible cavitation cones is a function of the cavitation number. Likewise, the derived formulae for entrainment and fictitious displacement include this parameter.

7 Recommendation

An important parameter in the derived formulae is the cavitation number the stagnation pressure increases firstly, with respect to the non-cavitating situation (σ_d). Probably this parameter depends, similar to the cavitation inception number, on nozzle geometry and nozzle diameter. It is recommended to investigate this dependency.

Acknowledgments These tests were conducted as part of a PhD study at Delft University of Technology, the Netherlands. They were

funded by the Dutch dredging companies Royal Boskalis Westminster NV and Van Oord Dredging and Marine Contractors BV. Their support is gratefully acknowledged.

Open Access This article is distributed under the terms of the Creative Commons Attribution Noncommercial License which permits any noncommercial use, distribution, and reproduction in any medium, provided the original author(s) and source are credited.

References

- Alehossein H, Qin Z (2007) Numerical analysis of Rayleigh–Plesset equation for cavitating water jets. *Int J Numer Method Eng* 72:780–807
- Berg Jvd, Ginneken Rv, Hilterman J, Vollebregt T (2006) Increasing the stagnation pressure of a submerged water jet. Ba-Thesis, Faculty Mechanical, Maritime and Materials Engineering, Delft University of Technology
- Brennen CE (1995) Cavitation and bubble dynamics. Oxford University Press, Oxford
- Fischer HB, List E, Koh R, Imberger J, Brooks N (eds) (1979) Mixing in inland and coastal waters. Academic Press, London
- Fondse H, Leijdens H, Ooms G (1983) On the influence of the exit conditions on the entrainment rate in the development region of a free, round, turbulent jet. *Appl Sci Res* 50:355–375
- Gopalan S, Katz J, Knio O (1999) The flow structure in the near field of jets and its effect on cavitation inception. *J Fluid Mech* 398:1–43
- Lienhard JH, Stephenson JM (1966) Temperature and scale effects upon cavitation and flashing in free submerged jets. *J Basic Eng* 88:525–532
- Nobel AJ, Cornelisse JM, Rhee Cv (2010) High speed recordings of a moving submerged water jet in cohesive soil. In: 20th International conference on jet cutting, Graz. BHR-group
- O’Hern T, d’Agostino L, Acosta A (1988) Comparison of holographic and coulter counter measurements of cavitation nuclei in the ocean. *ASME J Fluids Eng* 110:200–207
- Ooi KK (1985) Scale effects on cavitation inception in submerged water jets. *J Fluid Mech* 151:367–390
- Peng G, Fujikawa S (2006) Numerical study of cavitating turbulent flows in a starting submerged water jet. In: 6th International symposium on cavitation, pp 1–8
- Rajaratnam N (1976) Turbulent jets. Elsevier, Amsterdam
- Ran B, Katz J (1994) Pressure fluctuations and their effects on cavitation inception within water jets. *J Fluid Eng* 113:223–263
- Shen Z, Sun Q (1988) Study of pressure attenuation of a submerged non-free jet and a method of calculation for bottomhole hydraulic parameters. *SPE Drill Eng* 3:69–76
- Soyama H, Lichtarowicz A (1996) Cavitating jets—similarity correlations. *J Jet Flow Eng* 12:9–19
- Summers DA, Sebastian Z (1980) Considerations in the use of water jets to enlarge deep submerged cavities. In: 5th International symposium on jet cutting technology, pp 87–96
- Vinke FRS (2009) Water jets surrounded by an air film. Ms-Thesis, Faculty Civil Engineering and Geosciences, Delft University of Technology
- Weissenborn PK, Pugh RJ (1995) Surface tension and bubble coalescence phenomena of aqueous solutions of electrolytes. *Langmuir* 11:1422–1426
- Xing T, Frankel SH (2002) Effect of cavitation on vortex dynamics in a submerged laminar jet. *AIAA J* 40:2266–2276
- Yahiro T, Yoshida H (1974) On the characteristics of high speed water jet in the liquid and its utilization on the induction grouting method. In: 2nd International symposium on jet cutting technology, pp 41–63